Spectrochimica Acta Part B 142 (2018) 37–49

Contents lists available at ScienceDirect

Spectrochimica Acta Part B

journal homepage: www.elsevier.com/locate/sab

Fiber-optic laser-induced breakdown spectroscopy of zirconium metal in air: Special features of the plasma produced by a long-pulse laser

Ayumu Matsumoto [a,*], Hironori Ohba [a,b], Masaaki Toshimitsu [a], Katsuaki Akaoka [a], Alexandre Ruas [a], Tetsuo Sakka [c], Ikuo Wakaida [a]

[a] Collaborative Laboratories for Advanced Decommissioning Science, Japan Atomic Energy Agency, Tokai-mura, Naka-gun, Ibaraki 319-1195, Japan
[b] Tokai Quantum Beam Science Center, National Institutes for Quantum and Radiological Science and Technology, Tokai-mura, Naka-gun, Ibaraki 319-1106, Japan
[c] Department of Energy and Hydrocarbon Chemistry, Graduate School of Engineering, Kyoto University, Nishikyo-ku, Kyoto 615-8510, Japan

ARTICLE INFO

Article history:
Received 15 August 2017
Received in revised form 12 December 2017
Accepted 23 January 2018
Available online xxxx

Keywords:
Fukushima Daiichi decommissioning
Long-pulse laser
Fiber-optic LIBS
Zirconium

ABSTRACT

The decommissioning of the Tokyo Electric Power Company (TEPCO) Fukushima Daiichi Nuclear Power Plant is an essential issue in nuclear R&D. Fiber-optic laser-induced breakdown spectroscopy (Fiber-optic LIBS) could be used for in-situ elemental analysis of the inside of the damaged reactors. To improve the performances under difficult conditions, using a long-pulse laser can be an efficient alternative. In this work, the emission spectra of zirconium metal in air obtained for a normal-pulse laser (6 ns) and a long-pulse laser (100 ns) (wavelength: 1064 nm, pulse energy: 12.5 mJ, spot diameter: 0.35 mm) are compared to investigate the fundamental aspects of fiber-optic LIBS with the long-pulse laser. The spectral features are considerably different: when the long-pulse laser is used, the atomic and molecular emission is remarkably enhanced. The enhancement of the atomic emission at the near infrared (NIR) region would lead to the observation of emission lines with minimum overlapping. To understand the differences in the spectra induced respectively from the normal-pulse laser and the long-pulse laser, photodiode signals, time-resolved spectra, plasma parameters, emission from the ambient air, and emission regions are investigated, showing the particular characteristics of the plasma produced by the long-pulse laser.

1. Introduction

The Tokyo Electric Power Company (TEPCO) Fukushima Daiichi Nuclear Power Plant was seriously damaged by the tsunami caused by the earthquake on March 11, 2011 in Japan. The nuclear fuels are considered to be melted with the fuel cladding tubes, the control rods, the structural materials, the concretes, etc. The removal of the nuclear fuel debris from the inside of the damaged reactors where the radiation level is extremely high is very challenging. Various approaches have been used to improve the understanding of the reactor conditions, e.g. accident sequence analyses [1–8], evaluation of simulated debris [9–14], cosmic ray muon tomography [15,16], and internal observation with small robots (e.g. ref. [17]). However, at present, the elemental composition of the debris has yet to be confirmed.

Fiber-optic laser-induced breakdown spectroscopy (fiber-optic LIBS) is an in-situ analytical technique in which the emission spectroscopy of the laser ablation plasma is performed through an optical fiber cable. Because of the capability of remote analysis and the flexibility of the cable, this technique has been applied to various fields [18–25] including nuclear power plant [19]. The transmission of the laser pulse and the plasma emission through the cable enables us to probe into the damaged reactors without radiation exposure to the field workers and the electronics. Our group has developed a fiber-optic LIBS instrument combined with a radiation-resistant optical fiber and successfully analyzed simulated debris [26].

In practice, the head of the focusing optics should be miniaturized to access the inside of the damaged reactors with the narrow spaces. This limits the performances of the laser focusing and the light collection. To improve the analytical capability, the enhancement of the output energy and the plasma emission is important. Also, the analysis of submerged materials [26] and contaminated water [27] is required, because a part of the damaged reactors is underwater. In a previous work, a gas-flow system was employed [26], which enables us to analyze solid surfaces by ejecting the surrounding water [19,28]. However, the analysis of sediments and suspended particles is difficult to perform with the previous instrument.

In this context, the use of a long-pulse laser (~100 ns) instead of a commonly used normal laser (~10 ns) is a promising candidate. The peak power of the long-pulse laser is much lower than that of the normal-pulse laser for a same pulse energy, which allows the delivering of a higher laser energy to samples through the fiber without damaging it. Also, Sakka et al. have reported that a longer pulse duration gives intense and narrow emission lines in the water-confined geometry [29].

* Corresponding authors.
E-mail address: matsumoto.ayumu@eng.u-hyogo.ac.jp (A. Matsumoto).

https://doi.org/10.1016/j.sab.2018.01.012
0584-8547/

Because of its single-pulse scheme and applicability to high pressure environments [25,30,31], long-pulse LIBS has been widely studied for the analysis underwater (e.g. refs [32–39].).

However, the number of reports related to long-pulse LIBS in gaseous phase is still lacking. For example, Yamamoto et al. have evaluated the practicability of an acousto-optic (AO) Q-switched long-pulse laser (150 ns) with a pulse energy of ~10 mJ and a repetition rate up to 6 kHz for the analysis of aluminum, steel, soil samples, and surface contaminations [40]. Elnasharty has studied the effects of the pulse duration on the analysis of aluminum samples using a long-pulse fiber laser (40–200 ns) with a pulse energy of 200 μJ and a repetition rate of 25 kHz [41]. In the present Fukushima Daiichi decommissioning application where the laser beam cannot be tightly focused, a higher pulse energy is important rather than a high repetition rate, which can be achieved by an electro-optic (EO) Q-switched long-pulse laser. The CO_2 laser (~100 ns) is also a common long-pulse laser [42–47], but the longer wavelength (10.6 μm) is significantly absorbed by water and special materials are needed for the optics. Since the transmission property of the radiation-resistant fiber is not deteriorated at the near infrared (NIR) region even in the high-radiation fields [48], the wavelength of 1064 nm is a more reasonable choice. Zirconium metal is an important material to evaluate before analyzing more complex systems, because it is a main component of the fuel cladding tubes [10,11,13].

In this context, the emission spectrum of zirconium metal in air is measured using an EO Q-switched long-pulse laser (100 ns) with a wavelength of 1064 nm. The spectrum is compared to that obtained by a normal-pulse laser (6 ns) keeping a same output energy of 12.5 mJ at a spot diameter of 0.35 mm. To understand the differences of the spectra, photodiode signals, time-resolved spectra, plasma parameters, emission from the ambient air, and emission regions are investigated.

2. Experimental

Fig. 1 shows the experimental setup for fiber-optic LIBS. In this work, a flash-lamp-pumped EO Q-switched Nd:YAG laser (Continuum, Minilite II) with a pulse duration of 6 ns and a diode-pumped EO Q-switched Nd:YAG laser (OK Lab. Co., Ltd., OKL-LIBSLPL-8000) with a pulse duration of 100 ns were used. The lasers were operated at a wavelength of 1064 nm and a repetition rate of 5 Hz. The pulse duration was measured at the output of the focusing optics.

The laser beam to be examined was introduced into a quartz fiber (Mitsubishi Cable Industries, Ltd., PVSMAMSL) (delivery fiber) with a core diameter of 1.0 mm, a numerical aperture (NA) of 0.12, and a length of 2.5 m through a plano-convex lens (focal length: 125 nm) in a home-made coupling optics inside an airtight box. To avoid the damage at the entrance and the inside of the fiber, the focusing position was shifted, i.e. the distance from the lens to the end face of the fiber was 155 mm. Also, to avoid air breakdown, the inside of the box was roughly evacuated using a dry pump (AS ONE corporation, LMP-100) to reach a reduced pressure of 13.3 kPa. Note that the spatial distribution of the laser beam is considered to be averaged out by passing through the fiber cable and both the pulses show a top-hat beam profile. Thus, the difference of the transverse mode could be negligible in the present experiments.

The delivered beam was focused in a normal direction to the sample surface using a focusing optics (OK Lab. Co., Ltd., OKL-FPNC-IA2000) with a focal length of 80.34 mm, a reduction rate about 0.35, a working distance of 12.6 mm, and an outer diameter below 30 mm. The focusing optics was designed for collinear detection with a single fiber, and the chromatic aberration from 500 nm to 1064 nm was corrected. The distance between the focusing optics and the sample was previously adjusted so that the spot size of a He—Ne laser (wavelength: 632.8 nm) was minimum at the sample surface. The spot diameter was about 0.35 mm. The laser irradiation was performed keeping the output energy at 12.5 mJ for both the pulses (fluence: 13.0 J/cm^2, irradiance: 2.2 GW/cm^2 (6 ns) and 0.130 GW/cm^2 (100 ns)). In the present conditions, the input energy was sufficiently lower than the damage threshold of the delivery fiber for the 6-ns pulse laser, and the output energy was sufficiently higher than the ablation threshold of the sample for the 100-ns pulse laser.

As a sample, a zirconium metal plate (The Nilaco Corporation, ZR-493402, 99.2%) with a thickness of 0.50 mm was used. The target was cleaned in pure water and ethanol using an ultrasonic cleaner after the surface was polished by an emery paper (#1000). The sample was placed on an automatic rotating stage and the irradiation spot was changed shot-by-shot.

Emission spectroscopy was performed using an echelle spectrograph (Catalina Scientific Instruments, LLC, EMU-120/65 UV/VIS/NIR) equipped with an electron multiplying charge coupled device (EMCCD) camera (Raptor Photonics Limited, FA285B-CL) to adapt the numerous number of emission lines from nuclear reactor materials. In echelle spectrograph, horizontally-dispersed high-order diffraction light is vertically dispersed onto the detector for each diffraction order, and those with different wavelength region are connected, which gives high-resolution and wide range spectra. In EMCCD camera, the electrons are multiplied before the readout noise is generated, which enhances the signal without disturbing the spectral resolution. Although the focusing optics is designed for the collinear detection, the plasma emission was collected at the angle of about 30 degrees from the target surface using a light collector composed of two quartz plano-convex lenses (focal length: 40 mm, diameter of 25.4 mm) to observe the ultraviolet (UV) light. The collected light was delivered to the spectrograph through the fiber (SN402) (detection fiber) with a core diameter of 0.4 mm, which is an attachment of the spectrograph. In the spectral measurement, the delay time, the exposure time, the EMCCD gain, and the number of accumulation were set respectively to 1.0 μs, 50 μs, 2800 and 100. Note that 20% of the peak height at the falling edge of the laser pulse was defined as the delay time origin (t_d = 0 ns) to investigate the plasma evolution after the laser-plasma interaction. The recorded images were converted to intensity curves within a wavelength range from 190 to 1100 nm and a step width (interval between adjacent pixels) of 0.015 nm. In this work, a grating cassette HR1: UV/VIS/NIR with a slit width of 14 μm and a slit height of 41 μm

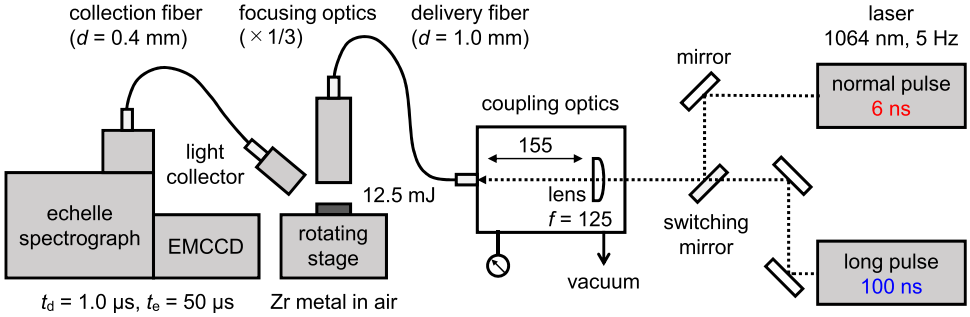

Fig. 1. Experimental setup for fiber-optic LIBS.